Synchronization in networks of spatially extended systems

Anastasiya E. Filatova,[1,a)] Alexander E. Hramov,[1,b)] Alexey A. Koronovskii,[1,c)] and Stefano Boccaletti[2]
[1]*Faculty of Nonlinear Processes, Saratov State University, Astrakhanskaya str., 83, Saratov, 410012, Russia*
[2]*CNR-Istituto dei Sistemi Complessi Via Madonna del Piano, 10 50019 Sesto Fiorentino (FI), Italy*
[3]*The Italian Embassy in Tel Aviv, Trade Tower, 25, Hamered St., 68125 Tel Aviv, Israel*

(Received 22 January 2008; accepted 20 May 2008; published online 30 June 2008)

Synchronization processes in networks of spatially extended dynamical systems are analytically and numerically studied. We focus on the relevant case of networks whose elements (or nodes) are spatially extended dynamical systems, with the nodes being connected with each other by scalar signals. The stability of the synchronous spatio-temporal state for a generic network is analytically assessed by means of an extension of the master stability function approach. We find an excellent agreement between the theoretical predictions and the data obtained by means of numerical calculations. The efficiency and reliability of this method is illustrated numerically with networks of beam-plasma chaotic systems (Pierce diodes). We discuss also how the revealed regularities are expected to take place in other relevant physical and biological circumstances. © *2008 American Institute of Physics*. [DOI: 10.1063/1.2940685]

The sophisticated collaborative dynamics of networking elements is nowadays of central interest of a very broad scientific community. In particular, the emergence and stability of collective (synchronized) dynamics in ensembles of elements interacting via a complex wiring of connections, has been the object of several studies aiming at discussing how synchronization properties can be actually enhanced by a proper weighting strategy on the strengths of the wiring connections. All previous works, however, were limited to the analysis of networks of dynamical systems with few degrees of freedom. In this paper, we extend the analysis to networks consisting of spatially extended dynamical systems, each one of them described by a set of partial differential equations, exhibiting spatiotemporal chaos. Such a representation seems, indeed, to describe more adequately a series of relevant situations encountered in technological and natural systems.

I. INTRODUCTION

The sophisticated collaborative dynamics of networking elements is nowadays of central interest for a very broad scientific community (see Ref. 1, and references therein). Complex networks are collections of nodes linked by a topologically complex wiring of connections. In most cases, they feature the so-called small world property, i.e., the fact that the path-length ℓ scales logarithmically with the network size N ($\ell \propto \log N$, in contrast to the linear scaling for regular lattices), and usually they display a clustering structure much more prominent than that characterizing random graph.

Recently, the dynamics of complex networks has been extensively investigated with regard to collective (synchronized) behaviors,[2,3] with special emphasis on the interplay between complexity in the overall topology and local dynamical properties of the coupled units. The usual case considered so far is that of networks of identical dynamical systems coupled by means of a complex wiring of connections. In this framework, several studies have shown how to enhance synchronization properties, by properly weighing the strengths of the connection wiring.[4–8]

At the same time, the majority of works devoted to complex network synchronization deals with node elements characterized by a small number of degrees of freedom,[9–13] although networks of spatiotemporal systems became the object of interest in the past years (e.g., the spatiotemporal networks has been studied in application to the chemical reactions[14,15] recently). In this paper we extend the study of synchronization phenomena in complex networks to the case of spatially extended coupled dynamical systems, i.e., in networks whose nodes are represented by dynamical systems, each one of them is described by partial differential equations.

The motivation is the fact that such a representation seems to more adequately describe a series of relevant situations encountered in natural (e.g., biological systems such as interacting cells[16]) and technological (e.g., laser arrays[17] or nonlinear antennas[18–21]) systems. For instance, in nonlinear antenna technologies, earlier studies of synchronous states were carried out[18–20] in the limit which the elements of the antenna were low dimensional nonlinear systems, but later it was shown that the use of spatially extended high-power microwave devices (such as backward wave oscillators,[22,23] Pierce diodes,[24–27] klystron generators,[28] gyrodevices,[29,30] etc.) is more appropriate in many practical circumstances.

Without lack of generality, we will concentrate on a network of spatially extended microwave beam-plasma objects (Pierce diodes), and develop a formalism that can be ex-

a)Electronic mail: rabbit@nonlin.sgu.ru.
b)Electronic mail: aeh@nonlin.sgu.ru.
c)Electronic mail: alkor@nonlin.sgu.ru.

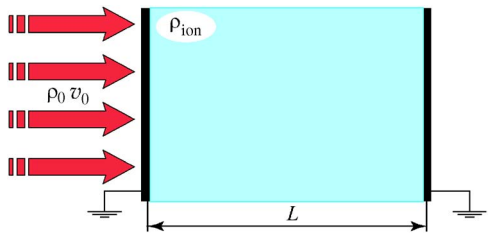

FIG. 1. (Color online) Schematic diagram of the Pierce diode.

tended to analyze the stability of the synchronous state in the generic situation of networking extended systems. It is important to notice that the Pierce diode is a well studied model of beam-plasma systems, demonstrating complex chaotic oscillations. In particular, the routes to spatial chaos,[24,25] pattern formation,[31] controlling chaos,[26,32–34] and synchronization[35,36] have been studied in great details.

The structure of this paper is the following: In Sec. II we discuss briefly the spatially extended nonlinear active system (the fluid model of Pierce diode) used as the node element of a complex network. The method of the stability analysis of networks whose nodes are represented by spatially extended dynamical systems is considered in Sec. III. Section IV is devoted to the method of the master stability function calculation in the spatially extended systems. The numerical results of the complex network calculation are discussed in Sec. V. The final conclusions are given in Sec. VI.

II. PIERCE DIODE

A Pierce diode[24,25,27,37] is schematically illustrated in Fig. 1, and consists of two infinite parallel plains pierced by a monoenergetic electron beam. Grids are grounded, with the distance between them being L. The charge density ρ_0 and electron velocity v_0 are constant at the system input. The region between the two plains is uniformly filled by neutralizing stationary ions, with density $|\rho_{ion}|$ being equal to the nonperturbed electron beam density $|\rho_0|$.

The dimensionless Pierce parameter $\alpha=\omega_p L/v_0$ determines the dynamics of the system (here ω_p is the electron beam plasma frequency, v_0 is the nonperturbed electron velocity, L is the distance between the diode plains). With $\alpha > \pi$, the so-called Pierce instability develops in the system and a virtual cathode is formed in the electron beam.[25,37] At the same time, in a narrow range of parameters near $\alpha \sim 3\pi$, the increase of the instability is suppressed by the nonlinearity and a reflectionless regime takes place in the electron beam.[25,27] In this case the system behavior may be described by the fluid equations[24,25,27] that give rise to various types of beam-plasma chaotic oscillations.[24,25,31,34]

The dynamics of the Pierce diode (in the fluid electronic approximation) is described by the self-congruent system of dimensionless Poisson, continuity, and motion equations,

$$\frac{\partial^2\varphi}{\partial x^2}=\alpha^2(\rho-1), \quad \frac{\partial\rho}{\partial t}=-\frac{\partial(\rho v)}{\partial x}, \quad \frac{\partial v}{\partial t}=-v\frac{\partial v}{\partial x}-\frac{\partial\varphi}{\partial x} \tag{1}$$

with boundary conditions $\varphi(0,t)=\varphi(1,t)=0$, $\rho(0,t)=1$, $v(0,t)=1$, where $\varphi(x,t)$ is the dimensionless potential of the electric field, $\rho(x,t)$ and $v(x,t)$ are the dimensionless density and velocity of the electron beam ($0\leqslant x\leqslant 1$), respectively. The dimensional variables (φ', ρ', v', x', t') are connected with the dimensionless ones as $\varphi'=(v_0^2/\eta)\varphi$, $\rho'=\rho_0\rho$, $v'=v_0 v$, $x'=Lx$, $t'=(L/v_0)t$, where η is the specific electron charge, v_0 and ρ_0 are the nonperturbed velocity and density of the electron beam.

The behavior of two Pierce diodes coupled both unidirectionally and mutually has been considered in Ref. 36. The synchronization to an external harmonic signal[35] and different types of chaotic synchronization[3,38–41] have been observed for the considered system.[36] Therefore, it seems to be likely that the network consisting of Pierce diodes may show the synchronous dynamics under the certain conditions, if the diodes are coupled in the same way, i.e., by the modulation of the potential value on the right bound of each system. The detailed description of such a network as well as the method of the analysis of the synchronous state stability are given in the next section.

III. STABILITY OF THE SYNCHRONOUS STATE OF THE COMPLEX NETWORK CONSISTING OF SPATIALLY EXTENDED SYSTEMS

Following a similar scheme used in Refs. 4, 39, and 42, we turn to develop the formalism of the stability analysis for a network of N Pierce diodes. The dynamics of the ith node of the network is described by the state $\mathbf{U}_i(x,t)=[\varphi_i(x,t),\rho_i(x,t),v_i(x,t)]^T$, with the dimensionless potential $\varphi_i(x,t)$ of the electric field, density $\rho_i(x,t)$, and velocity $v_i(x,t)$ of the electron beam being described by Eq. (1). Let us denote the evolution operator (1) of the ith node as

$$\hat{L}(\mathbf{U}_i)=0. \tag{2}$$

The influence of links between nodes results in the variation of the potential value $\varphi_i(1,t)$ at the right boundary of the ith Pierce diode (see Refs. 36 and 43 for detail) according to the states of the coupled node elements

$$\varphi_i(1,t)=-\sigma\sum_{j=1}^{N}G_{ij}\rho_j(1,t), \tag{3}$$

where σ is the coupling strength, $\rho_j(1,t)$ is the dimensionless electron beam density at the coordinate $x=1$ for the output grid of the jth diode. G is the Laplacian matrix of the network. As so, it is a symmetric zero row sum matrix $[G_{ij}$ $(i\neq j)$ is equal to 1 whenever node i is connected with node j and 0 otherwise, and $G_{ii}=-\Sigma_{j\neq i}G_{ij}]$, and it has a real spectrum of eigenvalues $\lambda_1\geqslant\cdots\geqslant\lambda_N$. The complete synchronization regime corresponds to the condition $\mathbf{U}_i(x,t)=\mathbf{U}_s(x,t)$, $\forall i$, with the boundary condition (3) taking the form $\varphi_i(1,t)=\varphi_s(1,t)=0$, $\forall i$. The synchronous manifold always exists as an invariant one, but it may be stable or unstable. The dynamics inside this manifold coincides with the behavior of a single diode.

To examine the stability of the synchronous manifold of the network we have to consider the dynamics of the small spatial perturbations $\xi=(\xi^\varphi,\xi^\rho,\xi^v)^T$ of the synchronous state $\mathbf{U}_s$ for each node of the network. Initially, these perturbations can be chosen to be arbitrary (but small). In general, the evolution of the network may result in both the increase or

decrease of each of these perturbations, according to the topology of links between nodes, the coupling strength value, and control parameter values of Pierce diodes. In fact, independently of initial conditions, each of the spatial perturbations evolves to the spatio-temporal mode being characterized by the maximum value of the damping decrement (or increment of growth). The synchronous state $[\mathbf{U}_i(x,t)=\mathbf{U}_s(x,t), \forall i]$ is stable if and only if all perturbations ξ_i decrease.

As far as small perturbations $\xi=(\xi^\varphi,\xi^\rho,\xi^v)^T$ to the synchronous state $\mathbf{U}_s$ are concerned, the behavior of the ith node is described by $\hat{L}(\mathbf{U}_s+\xi_i)=0$ with boundary conditions

$$\varphi_i(1,t)+\xi_i^\varphi(1,t)=-\sigma\sum_{j=1}^{N}G_{ij}[\rho_j(1,t)+\xi_j^\rho(1,t)],$$
$$\rho_i(0,t)+\xi_i^\rho(0,t)=1,\quad v_i(0,t)+\xi_i^v(0,t)=1. \tag{4}$$

Taking into account the vanishingly small values of the perturbations of the synchronous state $\mathbf{U}_s$, the evolution operator (2) may be rewritten as $\partial\hat{L}(\mathbf{U}_s,\xi_i)=0$, where $\partial\hat{L}(\mathbf{U}_s,\xi_i)$ is the linearization of the evolution operator $\hat{L}(\cdot)$ in the vicinity of the synchronous state $\mathbf{U}_s(x,t)$, therefore, it is linear in the perturbation $\xi(x,t)$. For the considered Pierce diode model the linearized operator $\partial\hat{L}(\mathbf{U}_s,\xi)$ is

$$\frac{\partial^2\xi^\varphi}{\partial x^2}=\alpha^2\xi^\rho,$$
$$\frac{\partial\xi^\rho}{\partial t}=-\xi^\rho\frac{\partial v_s}{\partial x}-v_s\frac{\partial\xi^\rho}{\partial x}-\xi^v\frac{\partial\rho_s}{\partial x}-\rho_s\frac{\partial\xi^v}{\partial x}, \tag{5}$$
$$\frac{\partial\xi^v}{\partial t}=-v_s\frac{\partial\xi^v}{\partial x}-\xi^v\frac{\partial v_s}{\partial x}-\frac{\partial\xi^\varphi}{\partial x}.$$

According to Eqs. (3) and (4), the boundary conditions for the perturbation ξ_i take the form

$$\xi_i^\varphi(1,t)=-\sigma\sum_{j=1}^{N}G_{ij}\xi_j^\rho(1,t),$$
$$\xi_i^\rho(0,t)=0,\xi_i^v(0,t)=0. \tag{6}$$

After diagonalization of the matrix G, the stability of the synchronous state $[\mathbf{U}_i(x,t)=\mathbf{U}_s(x,t),\forall i]$ is determined by the N evolution operators

$$\partial\hat{L}(\mathbf{U}_s,\varsigma_i)=0 \tag{7}$$

with boundary conditions

$$\varsigma_i^\varphi(1,t)=-\sigma\lambda_i\varsigma_i^\rho(1,t),\quad \varsigma_i^\rho(0,t)=0,\quad \varsigma_i^v(0,t)=0. \tag{8}$$

Equations (7) and (8) differ from each other only by the eigenvalues $\lambda_1\geqslant\cdots\geqslant\lambda_N$ of G.

IV. SPATIAL MASTER STABILITY FUNCTION

As it was mentioned above, the synchronous state $[\mathbf{U}_i(x,t)=\mathbf{U}_s(x,t),\forall i]$ is stable if all perturbations ς_i asymptotically vanish. We introduce here a quantity called the spatial master stability function (SMSF), which is analogous to the largest Lyapunov exponent in a low dimensional system.[39] Replacing $(-\sigma\lambda_i)$ by ν in Eq. (8), the behavior of SMSF Λ versus ν completely accounts for the linear stability of the synchronized state. Indeed, the synchronized state associated with $\lambda_1=0$ is stable when all the remaining equations (7) with boundary conditions (8) related with the other eigenvalues λ_i $(i=2,\ldots,N)$ gives rise to contracting equations. One has to consider the equation $\partial\hat{L}(\mathbf{U}_s,\varsigma)=0$ with parametric boundary conditions $\varsigma^\varphi(1,t)=\nu\varsigma_i^\rho(1,t)$, $\varsigma^\rho(0,t)=0$, $\varsigma^v(0,t)=0$ and analyze its stability properties. As such, a system is spatially extended, and is characterized by an infinite number of Lyapunov exponents. Nevertheless, the stability of the synchronous state $\mathbf{U}_s$ is determined uniquely by the sign of the largest Lyapunov exponent which can always be found by monitoring the temporal behavior of the perturbation norm $\|\xi\|$. Therefore, one has to obtain the dependence of the largest Lyapunov exponent Λ on the parameter ν.

$\Lambda(\nu)$ may be negative for a finite interval of ν-parameter values $I_{st}=(\nu_1;\nu_2)$ or for an infinite one $(\nu_2=\infty)$ just as the largest Lyapunov exponent does in Ref. 39. The stability condition is satisfied if the whole set of eigenvalues λ_i $(i=2,\ldots,N)$ multiplied by the same σ falls into the stability interval I_{st}, i.e., when conditions $\sigma|\lambda_2|>\nu_1$ and $\sigma|\lambda_N|<\nu_2$ take place simultaneously.

To analyze the stability of the synchronous state, we propose to use the average divergence rate of initial close states. Let our system be characterized by the state $\mathbf{U}(\mathbf{x},t_0)$ at time t_0. The distance $S(\mathbf{U}_1,\mathbf{U}_2)$ between two different states of the system may be defined as

$$S(\mathbf{U}_1,\mathbf{U}_2)=\left[\int_V\|\mathbf{U}_1(\mathbf{x})-\mathbf{U}_2(\mathbf{x})\|^2dV\right]^{1/2}. \tag{9}$$

Let us now consider the evolution of two systems with close (but different) initial conditions $\mathbf{U}^0(\mathbf{x},t_0)$ and $\tilde{\mathbf{U}}^0(\mathbf{x},t_0)=\mathbf{U}^0(\mathbf{x},t_0)+\tilde{\xi}(\mathbf{x})$, where $\tilde{\xi}(\mathbf{x})$ is a random function, $S(\mathbf{U}^0,\tilde{\mathbf{U}}^0)=\epsilon$, with ϵ being vanishingly small. These two states evolve to $\mathbf{U}_1(\mathbf{x})$ and $\tilde{\mathbf{U}}_1(\mathbf{x})$ at time t_0+T, respectively. The relation $S(\mathbf{U}_1,\tilde{\mathbf{U}}_1)/\epsilon$ describes the growth (decay) of the perturbation $\tilde{\xi}(\mathbf{x})$ during the time interval T. One can redefine the perturbed state $\tilde{\mathbf{U}}_1(\mathbf{x})$ in such a way that its deviation from the nonperturbed one $\mathbf{U}_1(\mathbf{x})$ is equal to the initial value ϵ: $\tilde{\mathbf{U}}_1^0(\mathbf{x})=\epsilon\tilde{\mathbf{U}}_1/S(\mathbf{U}_1,\tilde{\mathbf{U}}_1)$. Repeating this algorithm M times one can find the variation of the perturbation for M iteration $P_M=\Pi_{k=1}^M S(\mathbf{R}_k,\tilde{\mathbf{R}}_k)/\epsilon$. The value of the SMSF is given by

$$\Lambda=\frac{1}{MT}\ln P_M=\frac{1}{MT}\sum_{k=1}^{M}\ln\frac{S(\mathbf{R}_k,\tilde{\mathbf{R}}_k)}{\epsilon}. \tag{10}$$

SMSF (10) is positive if the small perturbation $\tilde{\xi}(\mathbf{x})$ brought into the system increases with time, otherwise it is negative (the small perturbation decreases) or zero (the distance between perturbed and nonperturbed states of the system remains constant). It should be noted, that the increase (decrease) of perturbation $\tilde{\xi}(\mathbf{x})$ is exponential, therefore, SMSF behaves like a Lyapunov function. In general, if the problem under study allows us to obtain the dispersion relation $\lambda(k)$,

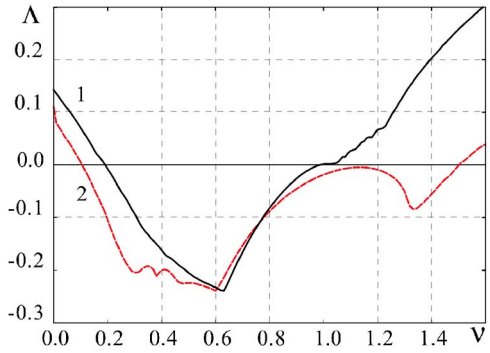

FIG. 2. (Color online) The dependencies of SMSF on parameter ν for $\alpha_1=2.858\pi$ (curve 1) and $\alpha_2=2.864\pi$ (curve 2). In the region of the negative values of the ν-parameter, SMSF dependencies are positive for both the $\alpha_{1,2}$ control parameter values and all values of ν.

the value of the SMSF coincides with the maximal value of the real part of the eigenvalues, i.e., $\Lambda=\max_k \mathrm{Re}\,\lambda(k)$.[44]

V. NUMERICAL RESULTS

In this section we consider the numerical results concerning the dynamics of the networks of Pierce diodes. We move now to two parameter values, i.e., $\alpha_1=2.858\pi$ and $\alpha_2=2.864\pi$ corresponding to different regimes of chaotic behavior of a single Pierce diode.[36] The dependencies of SMSF on the parameter ν are shown in Fig. 2. Based on these results, one can predict the coupling region for which a network of Pierce diodes would display a stable synchronization regime.

As a pair of mutually coupled Pierce diodes is the simplest network one can imagine, let us start with this elementary case. In this system the node elements $\mathbf{U}_{1,2}$ are coupled by means of a the coupling matrix

$$G=\begin{pmatrix}-1 & 1\\ 1 & -1\end{pmatrix}. \tag{11}$$

It was found (see Ref. 36) that the complete synchronization regime occurs for coupling strengths $\sigma\geqslant\sigma_c^{\alpha_1}=0.09$ for α_1 and $\sigma\geqslant\sigma_c^{\alpha_2}=0.05$ for α_2, respectively. It is easy to see that the eigenvalues of G are $\lambda_1=0$ and $\lambda_2=-2$. Therefore, in this case the ν-parameter is equal to 2σ.

One can see from Fig. 2 that SMSF becomes negative when the condition $\nu\approx 2\sigma_c^{\alpha_1}$ is satisfied if the value of Pierce parameter is α_1. Similarly, if the Pierce parameter value is α_2 SMSF crosses zero in the point $\nu\approx 2\sigma_c^{\alpha_2}$. Notice that SMSF is negative only for values of ν-parameter belonging to the interval $(\nu_1^{\alpha_{1,2}},\nu_2^{\alpha_{1,2}})$, $\nu_1^{\alpha_1}\approx 0.18$, $\nu_2^{\alpha_1}\approx 0.99$, $\nu_1^{\alpha_2}\approx 0.1$, $\nu_2^{\alpha_2}\approx 1.5$. Therefore, if the coupling strength σ exceeds $\sigma_2^{\alpha_{1,2}}=\nu_2^{\alpha_{1,2}}/|\lambda_2|$, the synchronization regime is destroyed. For the selected $\alpha_{1,2}$ the upper boundaries of the synchronous regime are $\sigma_2^{\alpha_1}=0.495$ and $\sigma_2^{\alpha_2}=0.750$, respectively.

In the direct simulations of the dynamics of coupled Pierce diodes, the appearance of a synchronous state can be monitored by looking at the vanishing of the time average (over a window T) synchronization error[5]

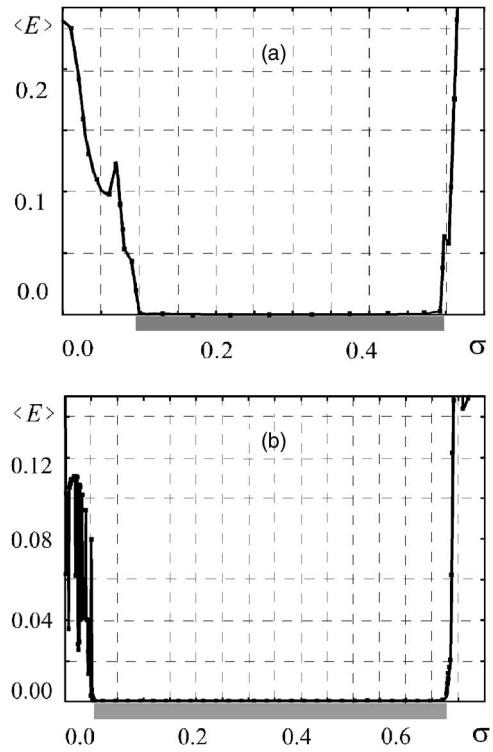

FIG. 3. The synchronization error $\langle E\rangle$ (see the text of work for detail) vs the coupling strength σ for the two mutually coupled Pierce diodes with $\alpha_1=2.858\pi$ (a) and $\alpha_2=2.864\pi$ (b). The theoretical predictions of the synchronization regime areas based on the consideration of SMSF are shown by the gray rectangles.

$$\langle E\rangle=\frac{1}{T(N-1)}\sum_{j>1}\int_t^{t+T} e_{j,1}(t')dt', \tag{12}$$

where

$$e_{i,j}(t)=\int_0^1 (|\varphi_i-\varphi_j|+|\rho_i-\rho_j|+|v_i-v_j|)dx \tag{13}$$

is the instantaneous spatially averaged synchronization error between $\mathbf{U}_{i,j}(x,t)$ of the ith and jth element of the network.

In the present case, the synchronization error may be rewritten as

$$\langle E\rangle=\frac{1}{T}\int_t^{t+T} e_{2,1}(t')dt'. \tag{14}$$

The synchronization errors $\langle E\rangle$ for two unidirectionally coupled Pierce diodes are shown in Figs. 3(a) and 3(b). One can see that the coupling strength values $\sigma_{1,2}^{\alpha_{1,2}}$ corresponding to the destruction of the complete synchronization regime are in excellent agreement with the theoretical predictions obtained by means of SMSF consideration for both values of the Pierce parameter $\alpha_{1,2}$.

The next examples of the networks of the spatially extended chaotic systems are (i) the square (5×5) lattice and (ii) the small world network. Both these networks consists of 25 Pierce diodes with the Pierce parameter value being selected as α_1. For the lattice the minimal nonzero eigenvalue of the coupling matrix G is $\lambda_{25}\approx -19.64$, the maximal one, $\lambda_2\approx -7.61$, whereas for the small-world network these ei-

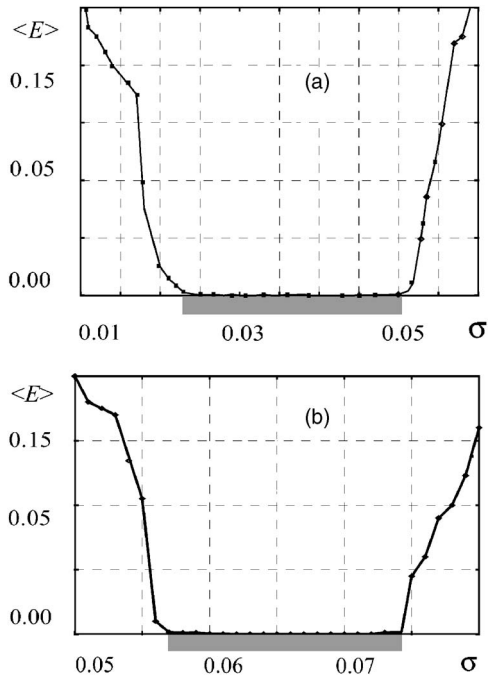

FIG. 4. The synchronization error $\langle E\rangle$ vs the coupling strength σ for the networks consisting of 25 coupled Pierce diodes with Pierce parameter $\alpha_1 = 2.858\pi$. (a) Corresponds to the lattice, and (b) to the small-world network, respectively. The theoretical predictions of the synchronization regime area based on the consideration of SMSF is shown by the gray rectangle.

genvalues are $\lambda_2 \approx -3.16$ and $\lambda_{25} \approx -13.29$, respectively. Correspondingly, one can expect that stability ranges of the synchronous regime are $\sigma \in (0.0570; 0.0745)$ for the small-word network and $\sigma \in (0.0237; 0.0504)$ for the lattice. From the direct numerical simulations of these networks and the synchronization error calculation we have obtained, that the small-world network is in the complete synchronization regime for the coupling strength values $\sigma \in (0.0570; 0.0744)$, whereas the synchronous state of the lattice is stable for $\sigma \in (0.0237; 0.0504)$. The corresponding dependencies of the synchronization error $\langle E\rangle$ on the coupling strength σ for these topologies are shown in Fig. 4. The theoretical predictions of the synchronization regime area based on the consideration of SMSF is shown by the gray rectangle. Again, one can see the excellent agreement of the results calculated numerically with the theoretical predictions obtained by means of SMSF consideration for both topologies of networks.

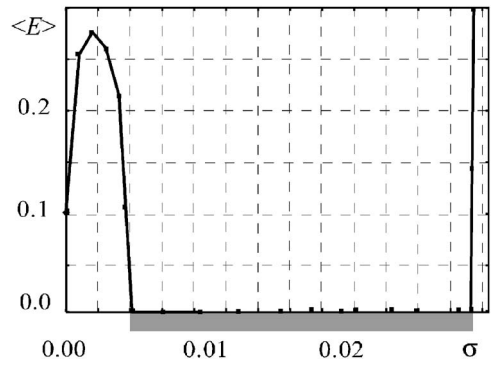

FIG. 5. The synchronization error $\langle E\rangle$ vs the coupling strength σ for the network consisting of 70 coupled Pierce diodes with Pierce parameter $\alpha_2 = 2.864\pi$. The theoretical predictions of the synchronization regime area based on the consideration of SMSF is shown by the gray rectangle.

Finally, we have also considered a network consisting of 70 Pierce diodes with a random symmetric zero row sum coupling matrix G. Since the distinction in the Pierce parameter values α_1 and α_2 does not cause the qualitative difference in the SMSF dependence on the ν-parameter (see Fig. 2), only one dependence of the synchronization error $\langle E\rangle$ on the coupling strength σ (for the value $\alpha_2 = 2.864\pi$) is given in this work in Fig. 5. The minimal nonzero eigenvalue of the coupling matrix G is $\lambda_{70} = -46.06$, the maximal one—$\lambda_2 = -24.42$. The synchronous regime for such a network should be observed in the range of the coupling strength values $\sigma \in (0.0041; 0.0326)$. The synchronization error for this network is shown in Fig. 5, the coupling strength value range $\sigma \in (\sigma_1; \sigma_2)\sigma_1 = 0.0043$ and $\sigma_2 = 0.0325$ where the complete synchronization regime takes place being shown by the gray rectangle.

The boundaries of the network synchronization regime for the different values of Pierce parameter α can be found in Table I. The critical values $\sigma_{1,2}^{\mathrm{SMSF}}$ and $\sigma_{1,2}^{\mathrm{net}}$ corresponding to the boundaries of the synchronous state obtained by both the SMSF calculation and direct numerical simulation of the network consisting of 70 Pierce diodes are given in this table for the different values of the Pierce parameter. The coupling matrix G is the same as before. The normalized difference

$$\delta_{1,2} = 2\frac{|\sigma_{1,2}^{\mathrm{SMSF}} - \sigma_{1,2}^{\mathrm{net}}|}{\sigma_{1,2}^{\mathrm{SMSF}} + \sigma_{1,2}^{\mathrm{net}}} \tag{15}$$

between boundary values obtained by both methods (given in percents) show the excellent agreement between these ap-

TABLE I. The boundaries of the synchronization of the network with the random coupling matrix.

α/π value	SMSF calculation		Numerical simulation		Error,%	
	σ_1^{SMSF}	σ_2^{SMSF}	σ_1^{net}	σ_2^{net}	δ_1	δ_2
2.858	0.007 40	0.021 50	0.007 41	0.021 45	0.135	0.233
2.859	0.007 65	0.020 84	0.007 68	0.020 82	0.295	0.084
2.860	0.007 41	0.021 71	0.007 42	0.021 70	0.028	0.024
2.861	0.006 14	0.028 22	0.006 16	0.028 22	0.327	0.003
2.862	0.004 91	0.028 44	0.004 93	0.028 43	0.328	0.024
2.863	0.004 91	0.031 05	0.004 94	0.031 03	0.453	0.061
2.864	0.004 14	0.032 57	0.004 31	0.032 51	0.148	0.002

proaches. A remarkable consistency between boundaries of synchronization obtained by means of the SMSF consideration and direct numerical calculations of the network dynamics is observed.

VI. CONCLUSION

We have considered the synchronization processes in the complex networks of spatially extended chaotic systems. This study was motivated by the fact that such a representation seems to be a more adequate description of many relevant phenomena occurring in natural systems. Moreover, the study of such networks allows us to better understand the fundamental aspects of chaotic synchronization including transition between different types of synchronous dynamics as well as interrelation between synchronization of spatially extended systems and synchronization of the systems with the small number of degree of freedom (e.g., the relationship between the generalized synchronization of the extended systems[45] and the GS regime of the oscillators with the small number of degree of freedom[46]).

The technique both for the stability analysis of the synchronous state in such networks and for the spatial master stability function calculation has been developed. The efficiency of the proposed approach has been illustrated by the consideration of the complex network of Pierce diodes. To verify the obtained theoretical predictions, we have performed the direct numerical simulation of the Pierce diode network dynamics and found an excellent agreement between the theoretical results and the data obtained by means of numerical calculations. Though the given technique has been explicitly derived here only for networks of beam-plasma chaotic systems (Pierce diodes), we expect that the very same mechanism can be observed in many other relevant circumstances, e.g., in the physiological[16,47–49] or physical systems.[17,50]

ACKNOWLEDGMENTS

This work has been supported by RFBR (Project Nos. 08-02-90002-Bel-a and 07-02-00044) and the Supporting program of leading Russian scientific schools (Project No. NSh-355.2008.2) and Doctor of Science (Project No. MD-1884.2007.2). We also thank the "Dynasty" Foundation.

[1] S. Boccaletti, V. Latora, V. Moreno, M. Chavez, and D.-U. Hwang, Phys. Rep. **424**, 175 (2006).
[2] L. M. Pecora and T. L. Carroll, Phys. Rev. Lett. **64**, 821 (1990).
[3] S. Boccaletti, J. Kurths, G. Osipov, D. L. Valladares, and C. S. Zhou, Phys. Rep. **366**, 1 (2002).
[4] M. Chavez, D.-U. Hwang, A. Amann, H. G. E. Hentschel, and S. Boccaletti, Phys. Rev. Lett. **94**, 218701 (2005).
[5] D.-U. Hwang, M. Chavez, A. Amann, and S. Boccaletti, Phys. Rev. Lett. **94**, 138701 (2005).
[6] A. E. Motter, C. Zhou, and J. Kurths, Phys. Rev. E **71**, 016116 (2005).
[7] C. Zhou, A. E. Motter, and J. Kurths, Phys. Rev. Lett. **96**, 034101 (2006).
[8] A. E. Motter, C. S. Zhou, and J. Kurths, Europhys. Lett. **69**, 334 (2005).
[9] S. N. Dorogovtesev and J. F. F. Mendes, *Evolution of Networks* (Oxford University Press, Oxford, 2003).
[10] R. Albert and A. L. Barabási, Rev. Mod. Phys. **74**, 47 (2002).
[11] D. J. Watts, *Small Worlds: The Dynamics of Networks between Order and Randomness* (Princeton University Press, Princeton, 1999).
[12] D. J. Watts and S. Strogatz, Nature (London) **393**, 440 (1998).
[13] I. Belykh, V. Belykh, and M. Hasler, Physica D **195**, 188 (2004).
[14] T. R. Chigwada, P. Parmananda, and K. Showalter, Phys. Rev. Lett. **98**, 074101 (2007).
[15] T. R. Chigwada, P. Parmananda, and K. Showalter, Phys. Rev. Lett. **95**, 038306 (2005).
[16] A. Gomez-Marin, J. García-Ojalvo, and J. M. Sancho, Phys. Rev. Lett. **98**, 168303 (2007).
[17] D. J. DeShazer, R. Breban, E. Ott, and R. Roy, Phys. Rev. Lett. **87**, 044101 (2001).
[18] H. Ito and E. Mosekilde, Trans. Inst. Electr. Eng. Jpn., Part A **113-A**, 365 (1993).
[19] W. L. Ditto, M. L. Spano, and J. L. Lindner, Physica D **86**, 198 (1995).
[20] B. K. Meadows, T. H. Heath, J. D. Neff, E. A. Brown, D. W. Fogliatti, M. Gabbay, V. In, P. Hasler, S. P. Deweerth, and W. L. Ditto, Proc. IEEE **90**, 882 (2002).
[21] R. A. York and Z. B. Popovic, *Active and Quasi-Optical Arrays for Solid State Power Combining. in Microwave and Optical Engineering* (Wiley, New York, 1997).
[22] N. S. Ginzburg, S. P. Kuznetsov, and T. N. Fedoseeva, Radiophys. Quantum Electron. **21**, 728 (1979).
[23] B. Levush, T. M. Antonsen, A. Bromborsky, W. R. Lou, and Y. Carmel, IEEE Trans. Plasma Sci. **20**, 263 (1992).
[24] B. B. Godfrey, Phys. Fluids **30**, 1553 (1987).
[25] H. Matsumoto, H. Yokoyama, and D. Summers, Phys. Plasmas **3**, 177 (1996).
[26] T. Klinger, C. Schroder, D. Block, F. Greiner, A. Piel, G. Bonhomme, and V. Naulin, Phys. Plasmas **8**, 1961 (2001).
[27] A. E. Trubetskov and A. E. Hramov, *Lectures on Microwave Electronics for Physicists* (Fizmatlit, Moscow, 2003).
[28] A. Shigaev, B. S. Dmitriev, Y. D. Zharkov, and N. M. Ryskin, IEEE Trans. Electron Devices **52**, 790 (2005).
[29] G. S. Nusinovich, A. N. Vlasov, and T. M. Antonsen, Phys. Rev. Lett. **87**, 218301 (2001).
[30] K. L. Felch, B. G. Danly, H. R. Jory, K. E. Kreischer, W. Lawson, B. Levush, and R. J. Temkin, Proc. IEEE **87**, 752 (1999).
[31] S. Kuhn and A. Ender, J. Appl. Phys. **68**, 732 (1990).
[32] H. Friedel, R. Grauer, and K. H. Spatschek, Phys. Plasmas **5**, 3187 (1998).
[33] A. E. Hramov and I. S. Rempen, Int. J. Electron. **91**, 1 (2004).
[34] A. E. Hramov, A. A. Koronovskii, and I. S. Rempen, Chaos **16**, 013123 (2006).
[35] M. S. Hur and H. J. Lee, Phys. Rev. E **58**, 936 (1998).
[36] R. A. Filatov, A. A. Hramov, and A. A. Koronovskii, Phys. Lett. A **358**, 301 (2006).
[37] J. R. Pierce, J. Appl. Phys. **15**, 721 (1944).
[38] A. E. Hramov and A. A. Koronovskii, Physica D **206**, 252 (2005).
[39] L. M. Pecora and T. L. Carroll, Phys. Rev. Lett. **80**, 2109 (1998).
[40] N. F. Rulkov, M. M. Sushchik, and L. S. Tsimring, Phys. Rev. E **51**, 980 (1995).
[41] A. E. Hramov and A. A. Koronovskii, Chaos **14**, 603 (2004).
[42] M. Dhamala, V. K. Jirsa, and M. Ding, Phys. Rev. Lett. **92**, 074104 (2004).
[43] A. E. Hramov, A. A. Koronovskii, P. V. Popov, and I. S. Rempen, Chaos **15**, 013705 (2005).
[44] A. E. Hramov, A. A. Koronovskii, and P. V. Popov, Phys. Rev. E **77**, 036215 (2008).
[45] A. E. Hramov, A. A. Koronovskii, and P. V. Popov, Phys. Rev. E **72**, 037201 (2005).
[46] A. E. Hramov, A. A. Koronovskii, and O. I. Moskalenko, Europhys. Lett. **72**, 901 (2005).
[47] A. E. Hramov, A. A. Koronovskii, I. S. Midzyanovskaya, E. Sitnikova, and C. M. Rijn, Chaos **16**, 043111 (2006).
[48] A. E. Hramov, A. A. Koronovskii, V. I. Ponomarenko, and M. D. Prokhorov, Phys. Rev. E **75**, 056207 (2007).
[49] A. E. Hramov, A. A. Koronovskii, V. I. Ponomarenko, and M. D. Prokhorov, Phys. Rev. E **73**, 026208 (2006).
[50] S. Boccaletti, E. Allaria, R. Meucci, and F. T. Arecchi, Phys. Rev. Lett. **89**, 194101 (2002).